Beyond the SM with nonlinearly realized gauge theories

Ruggero Ferrari

INFN, Sezione di Milano, via Celoria 16

Abstract:

1. Motivations [Stückelberg Mass Term (SMT)]

$$S_{YM} + M^2 \int d^4x \, Tr\big\{[gA_\mu - i\Omega\partial_\mu\Omega^\dagger]^2\big\}.$$

2. Lattice model for **massive** $SU(2)$ **Yang-Mills**

3. Lattice simulation.

4. Bound states? **(Preliminary)**

1. Introduction

The mass m is introduced in the action on the cubic lattice of size $N \equiv L^4$ with sites x and links μ

$$S_L = \frac{\beta}{2} \, \Re e \sum_{\square} Tr\{1 - U_{\square}\}$$

$$+ \frac{\beta}{2} m^2 \Re e \sum_{x\mu} Tr\{1 - \Omega(x)^{\dagger} U(x,\mu)\Omega(x+\mu)\} \ , \tag{1}$$

where the sum over the plaquette is the Wilson action. $U(x,\mu), \Omega(x) \in SU(2)$ and in the naive limit of zero lattice spacing a one gets a mass term $à\,la$ **Stückelberg** ($M^2 = a^{-2}m^2$)

$$S_{YM} + M^2 \int d^4x \, Tr\{[gA_{\mu} - i\Omega\partial_{\mu}\Omega^{\dagger}]^2\}. \tag{2}$$

2. Local and global gauge invariance

The action is invariant under the local-left transformations $g_L(x) \in SU(2)_L$ and the global-right transformations $g_R \in SU(2)_R$

$$SU(2)_L \begin{cases} \Omega'(x) = g_L(x)\Omega(x) \\ U'(x,\mu) = g_L(x)U(x,\mu)g_L^\dagger(x+\mu) \end{cases}, \quad SU(2)_R \begin{cases} \Omega'(x) = \Omega(x)g_R^\dagger \\ U'(x,\mu) = U(x,\mu) \end{cases} \quad (3)$$

We would like to stress the importance of this invariance property, in particular because in the nonrenormalizable continuum Minkowskean theory it is the starting point for the removal of the ultraviolet divergences of the loop expansion. In fact the invariance of the path integral measure ensures the validity of the LFE for the generating functionals [1].

3. Why a Lattice Theory and how?

The lattice formulation allows the exploration of the non-pertubative regime (as large energy phenomena, bound states). The present work is devoted to this exploration. The missing link to phenomenology is the identification of the line in the parameter space $(m^2(a), \beta(a))$ which allows the evaluation of the physical amplitudes. This can be achieved either by: i) evaluate relation among physical amplitudes where the dependence from $m^2(a)$ and $\beta(a)$ has been removed; ii) go in the perturbative regime and compare the amplitudes evaluated in the lattice and in the continuum.

4. Features of the Lattice Model

The statistics is performed by using the partition function

$$Z[\beta, m^2, N] = \sum_{\{U,\Omega\}} e^{-S_L} \tag{4}$$

It is well established that a Transition Line (TL) exists with end point at $\beta \simeq 2.2$ where energy and order parameter $(D = 4)$

$$\mathfrak{C} = \frac{1}{DN\beta}\frac{\partial}{\partial m^2}\ln Z = \frac{1}{2ND}\langle\Re e \sum_{x\mu} Tr\{\Omega^\dagger(x)U(x,\mu)\Omega(x+\mu)\}\rangle. \tag{5}$$

have an inflection point becoming steeper by increasing β. See Fig. 1
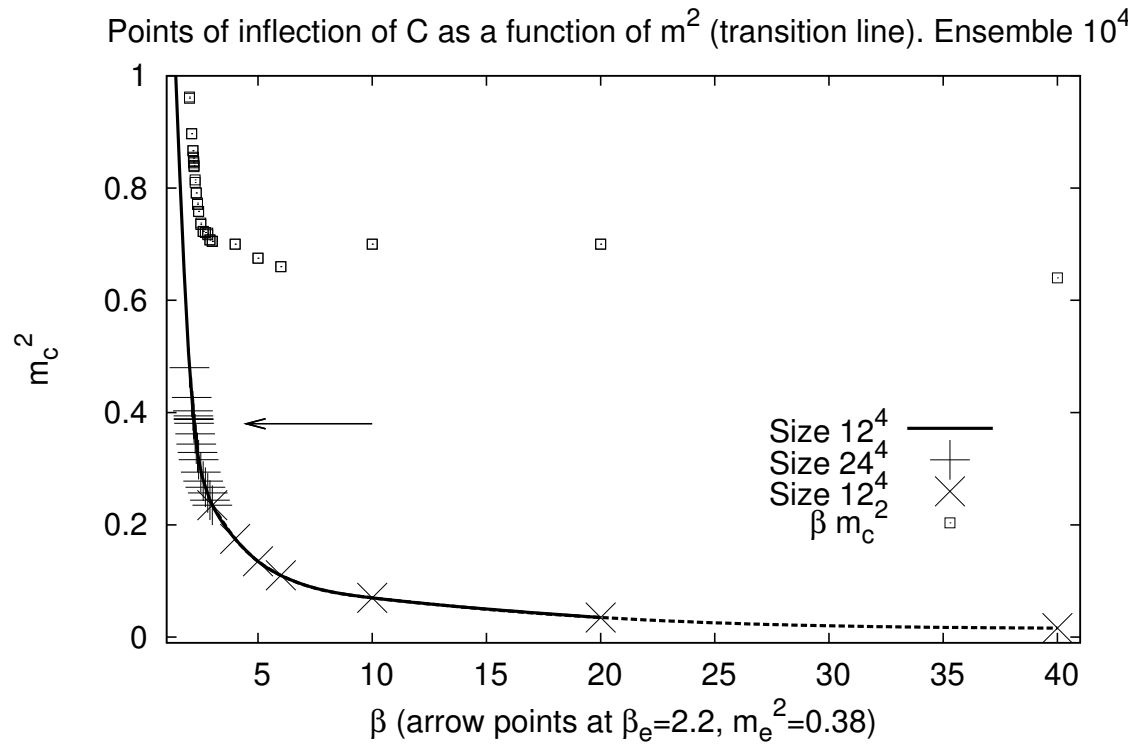
Figure 1: **The transition line. The arrow marks the position of the end point. In the figure data from previous analysis have been used and the statistical errors are not displayed since they are too small to be shown.**

5. Gauge invariant Fields

We study the two-point functions which can provide some information over the spectrum . The gauge invariant fields are very useful (τ_a are the Pauli matrices).

$$C(x, \mu) := \Omega^{\dagger}(x) U(x, \mu) \Omega(x + \mu) = C_0(x, \mu) + i \tau_a C_a(x, \mu). \quad (6)$$

By construction

$$C(x, \mu) \in SU(2). \quad (7)$$

$C(x, \mu)$ is invariant under local-left transformations , while under the global-right transformations they have $I = 0$ (C_0) and $I = 1$ components (C_a) (I is the isospin). One has

$$C_0(x, \mu)^2 + \sum_{a=1,3} C_a(x, \mu)^2 = 1. \quad (8)$$

6. Correlators: General Properties

In the deconfined region we expect the global-right symmetry to be implemented and therefore

$$\langle C_a(x, \mu) \rangle = 0$$

$$\langle C_a(x, \mu) C_b(y, \nu) \rangle = 0, \qquad if \ a \neq b. \tag{9}$$

Moreover the symmetry over four-dimensional finite rotations requires

$$\langle C_a(x, \mu) C_a(y, \nu) \rangle = 0, \qquad if \ \mu \neq \nu. \tag{10}$$

The equations (9) and (10) are satisfied by the numerical simulations to a reasonable level of accuracy.

7. Correlators: Energy Gaps

Consider the two-point function of the zero -three-momentum operator

$$C_j(t, \mu) = \frac{1}{L^{\frac{3}{2}}} \sum_{x_1, x_2, x_3} C_j(x_1, x_2, x_3, x_4, \mu)|_{x_4=t}, \quad j = 0, 1, 2, 3. \quad (11)$$

Then we evaluate the connected correlator

$$C_{jj', \mu\nu}(t) = \frac{1}{L} \sum_{t_0=1, L} \langle C_j(t + t_0, \mu) C_{j'}(t_0, \nu) \rangle_C. \quad (12)$$

The correlator is zero unless $j = j'$ and $\mu = \nu$. The spin one- and zero- amplitudes V and S are extracted by using the relation

$$C_{jj, \mu\nu}(t) = V_{jj}(\delta_{\mu\nu} - \delta_{\mu 4}\delta_{\nu 4}) + S_{jj}\delta_{\mu 4}\delta_{\nu 4}. \quad (13)$$

Very good fit of the data is obtained by using the function

$$g(t) = \frac{1}{2}(f(t) + f(L - t))$$
$$f(t) = b_1 e^{-m_1 t} + b_2 e^{-m_2 t}. \tag{14}$$

Two exponentials are needed only for $m \simeq m_c$, as we will illustrate shortly. Otherwise one single exponential is enough for the fit. For comparison the $\beta = 1.5$ single exponential is shown with the $\beta = 3$ two exponentials in Figs. 2 and 3.
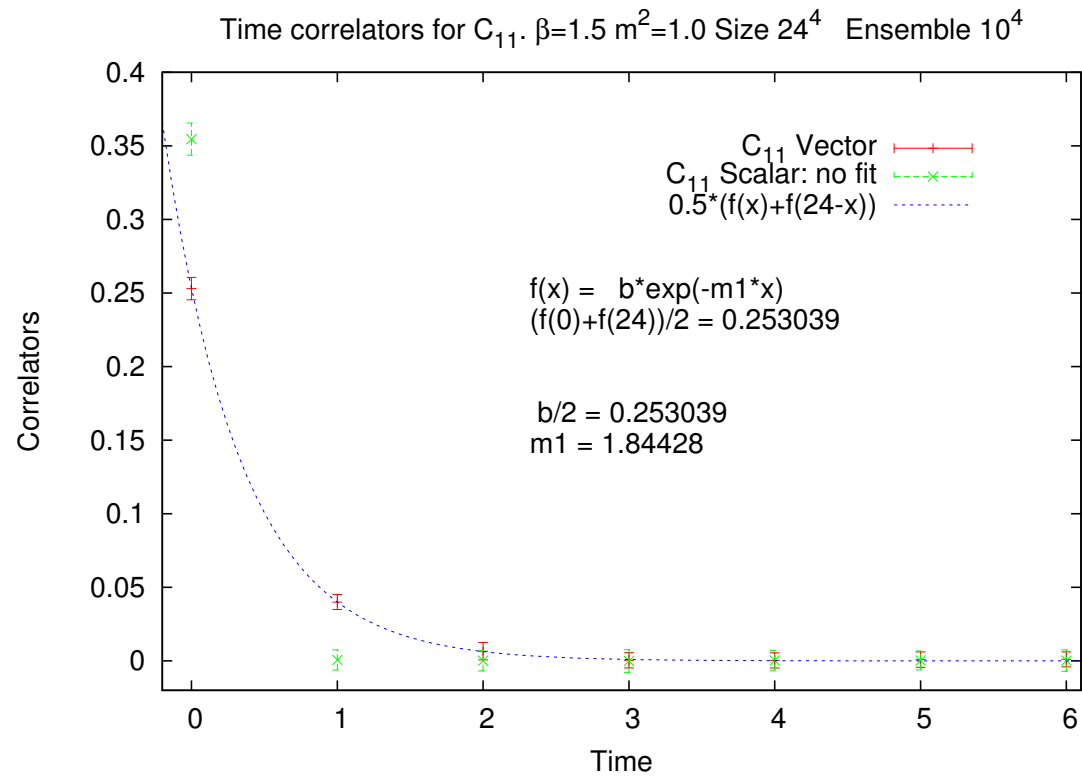
Figure 2: **A time correlator in the isovector channel where a single exponential is used. The mass m^2 is close to the TL at $m_c^2 \sim 0.9$.**

LC13, ECT* Trento, 19.9.2013
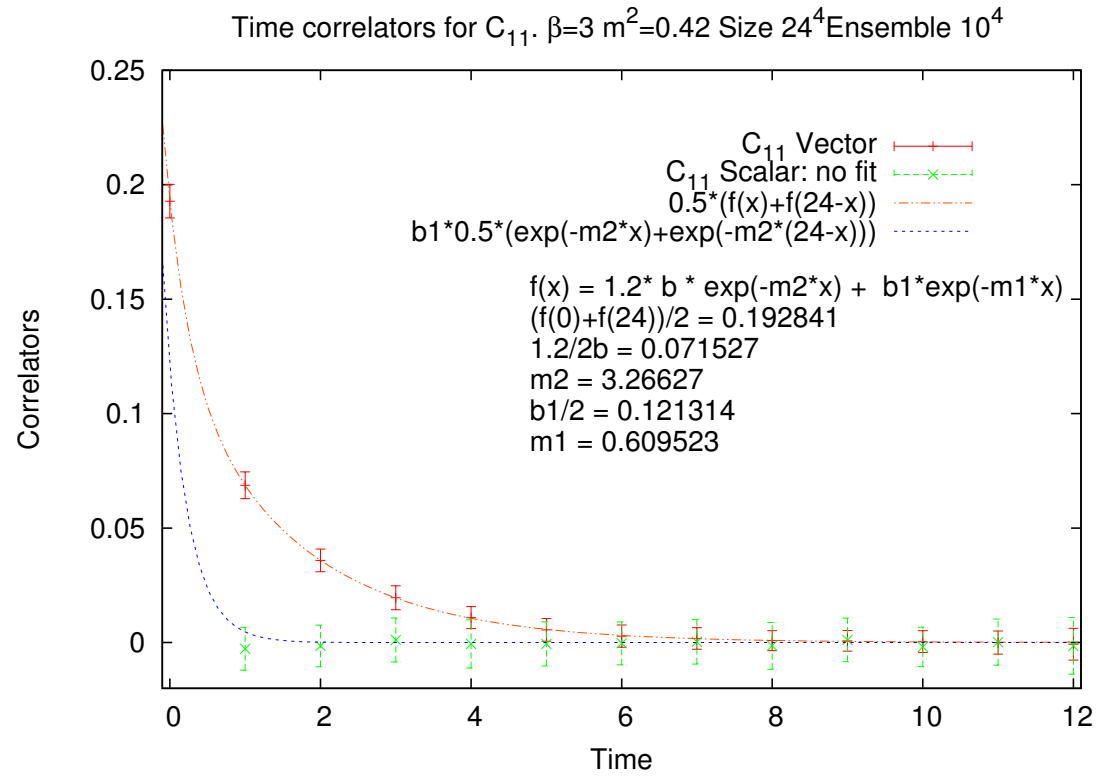
Figure 3: **A time correlator in the isovector channel where two exponentials are used. The mass m^2 is close to the TL at $m_c^2 \sim 0.231$. The figure shows the contribution of the large energy gap.**

LC13, ECT* Trento, 19.9.2013

8. The Spectrum for $\beta = 1.5$

We collect all the simulation data for $\beta = 1.5$. Interesting case since there is only one phase. We explore all three channels $I = 1, J = 1$ and $I = 0, J = 0, 1$. **Fig. 2**, **Fig. 3** and **Fig. 4** show that the single exponential fit is good and that there is at least one state for each channel. The $I = 1, J = 1$ is the candidate for the vector meson: its mass m_1 follows the bare curve $\sqrt{m^2}$.
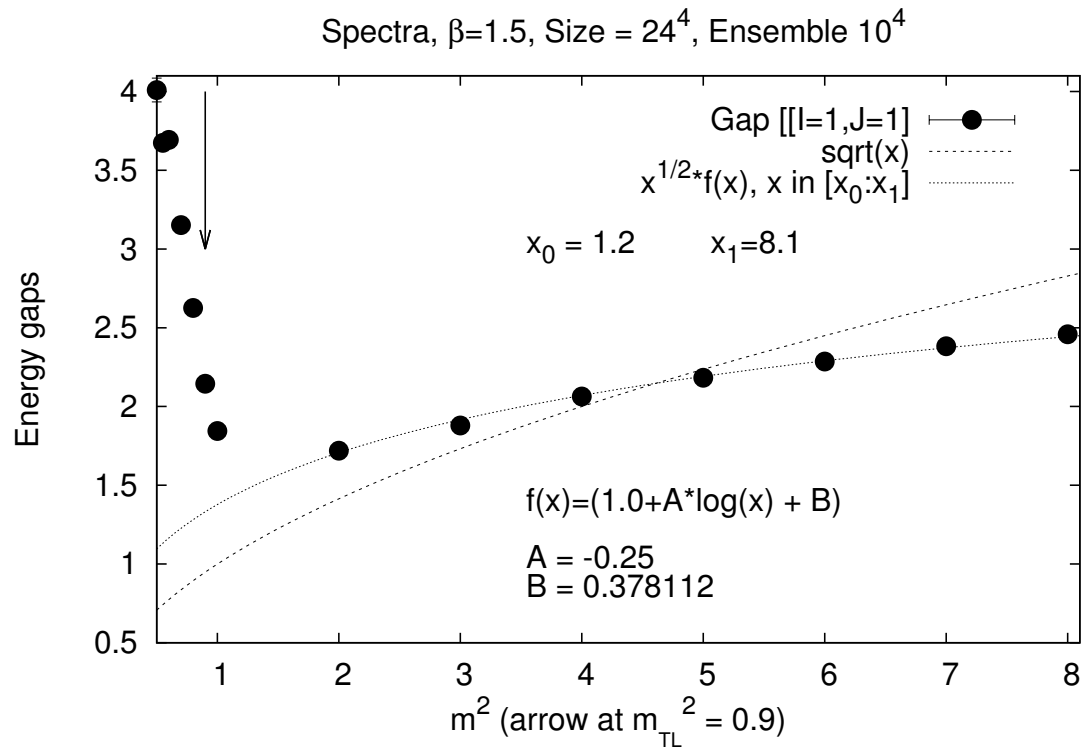
Figure 4: **Mass spectrum of the gauge vector meson for** $\beta = 1.5$.
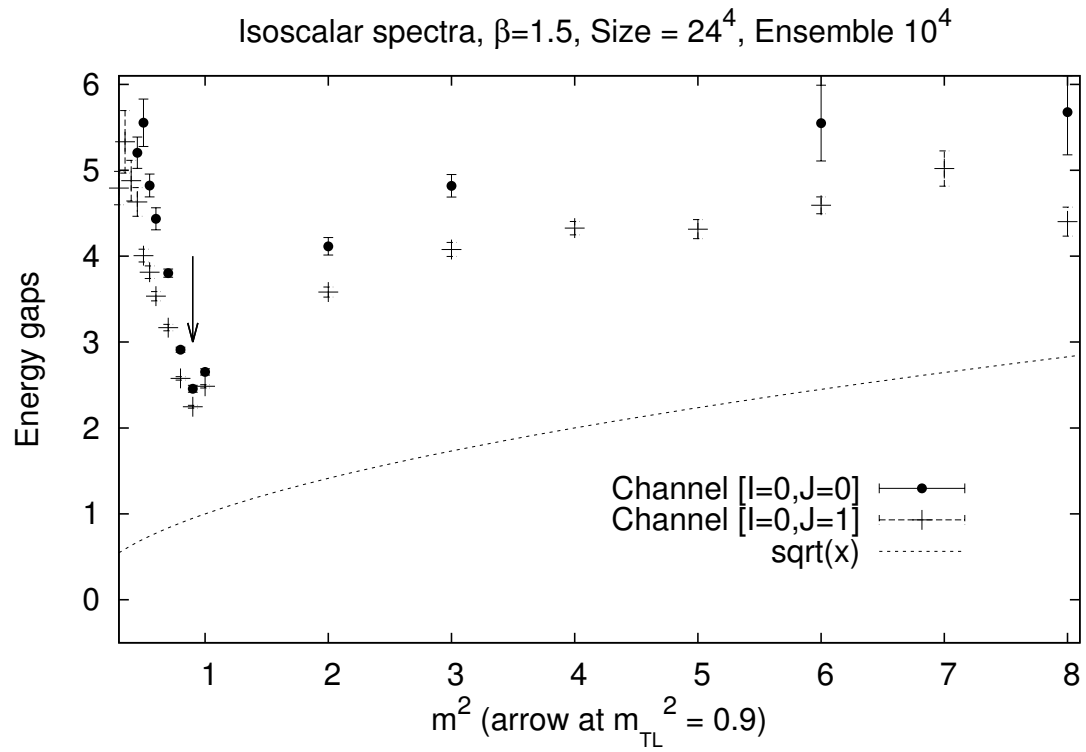
Figure 5: **Mass spectrum in the isoscalar channels** $(J = 0, 1)$ **for** $\beta = 1.5$.

9. The Spectrum for $\beta = 10$

For β above the end point the fit with two exponentials becomes necessary as m^2 approaches the m^2_{TL}. Typically (clearer in the isovector channel) there is a bifurcation point where one gap follows the bare value m and the other is very large. The weight of the larger gap becomes dominant for m^2 near m^2_{TL}. A series of Figures illustrates the phenomenon: for $I = 1, J = 1$ **Fig. 6**, for $I = 0, J = 0$ **Fig. 7**, for $I = 0, J = 1$ **Fig. 8**. By m^2 approaching m^2_c the weight of the large gap becomes dominant as shown in **Fig. 9** for $I = 1, J = 1$, **Fig. 10** for $I = 0, J = 0$ and **Fig. 11** for $I = 0, J = 1$.
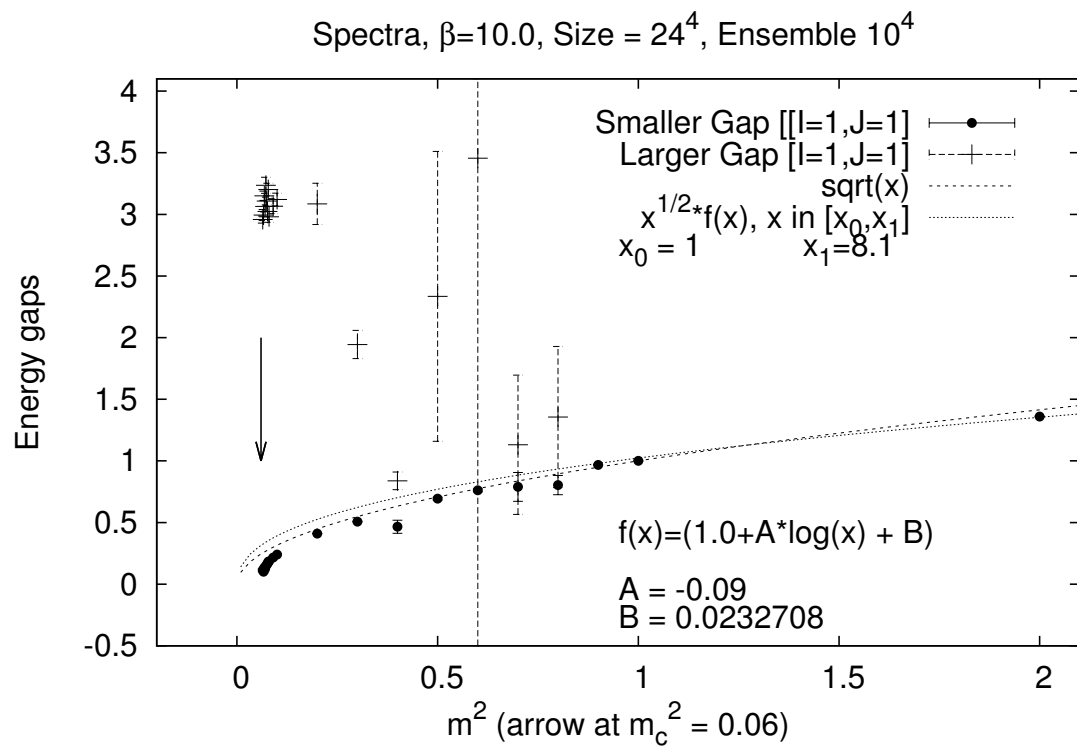
Figure 6: **Mass spectrum in the isovector channel $(J = 1)$ for $\beta = 10$.**
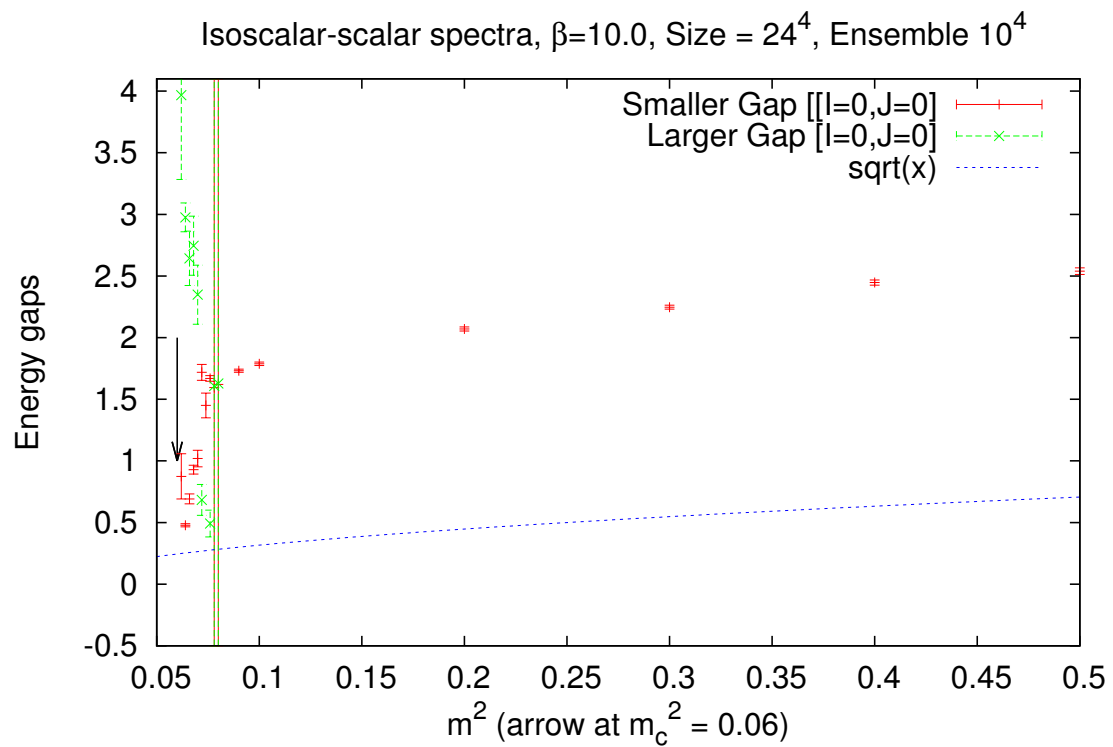
Figure 7: **Mass spectrum in the isoscalar channel** $(J = 0)$ **for** $\beta = 10$.
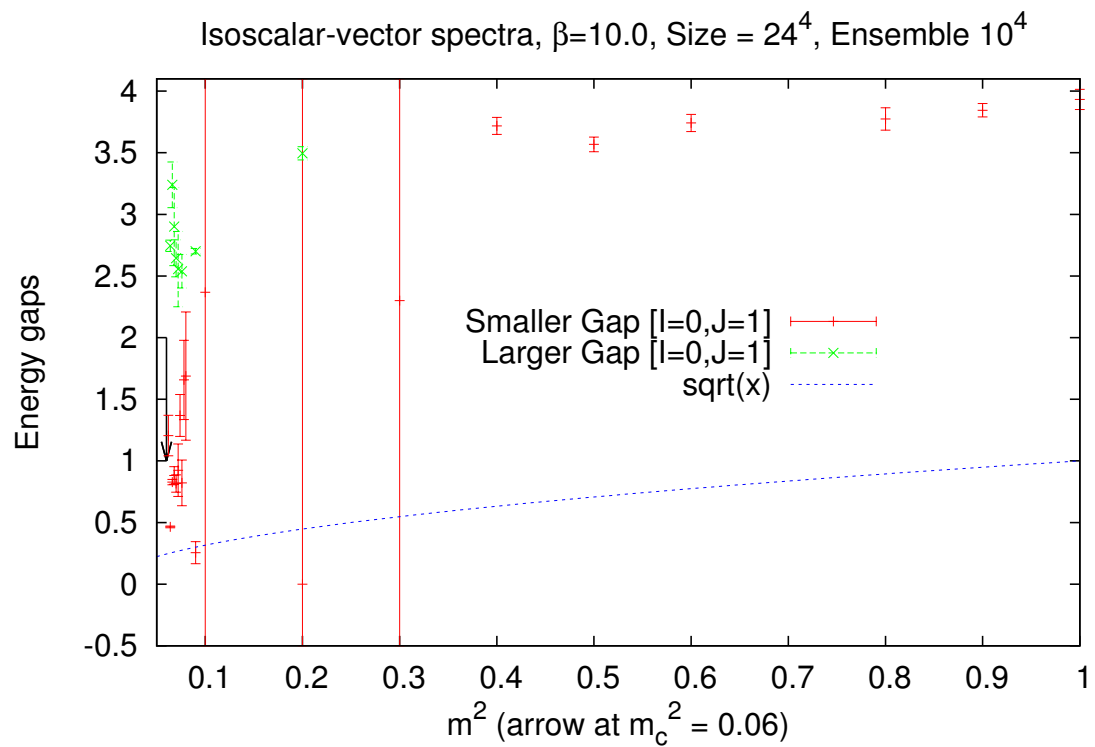
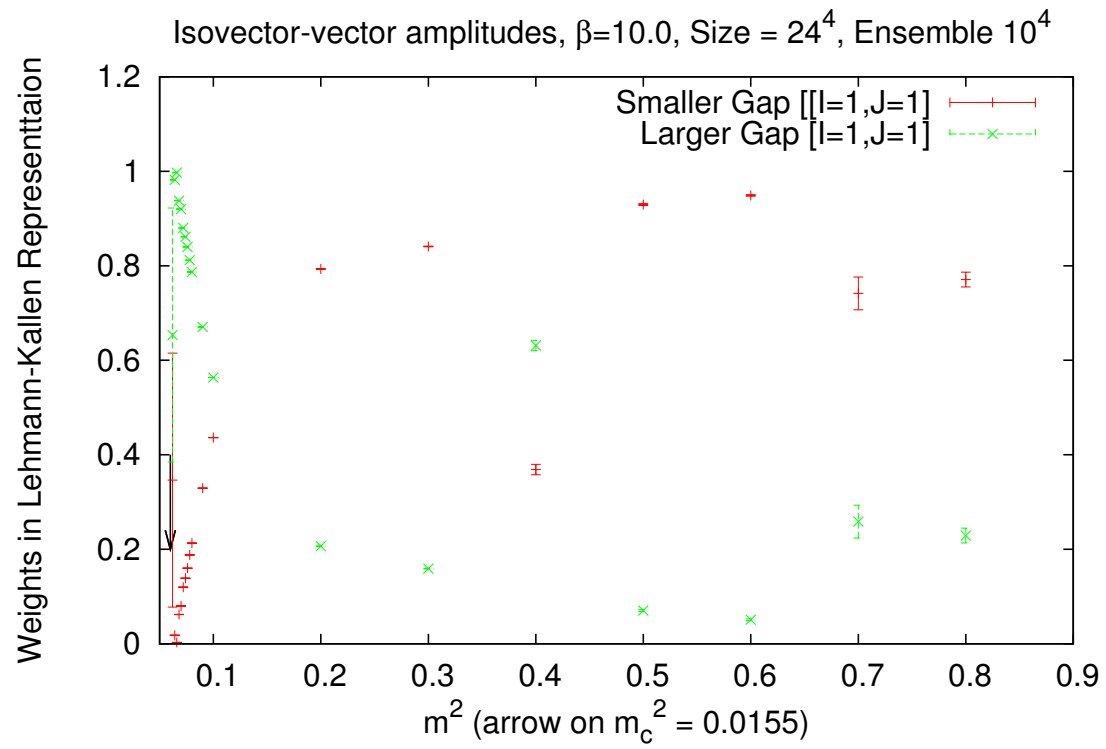Figure 8: **Mass spectrum in the isoscalar channel ($J = 1$) for $\beta = 10$.**

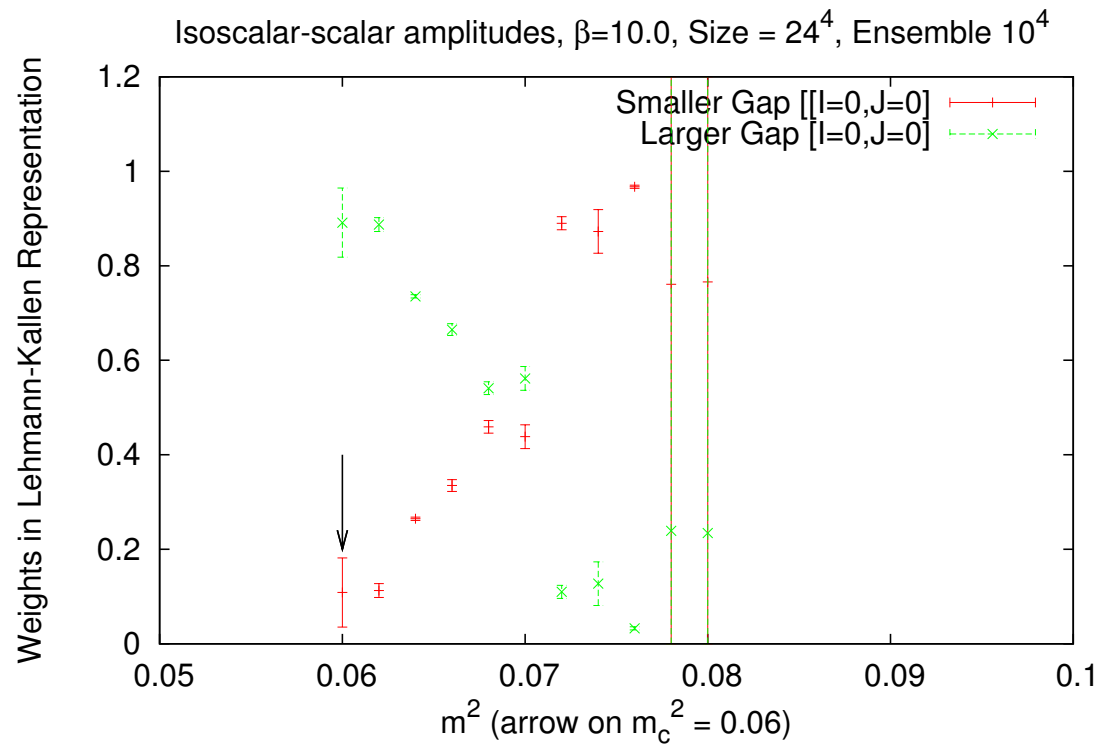Figure 9: **Weights in the isovector channel** $(J = 1)$ **for** $\beta = 10$.

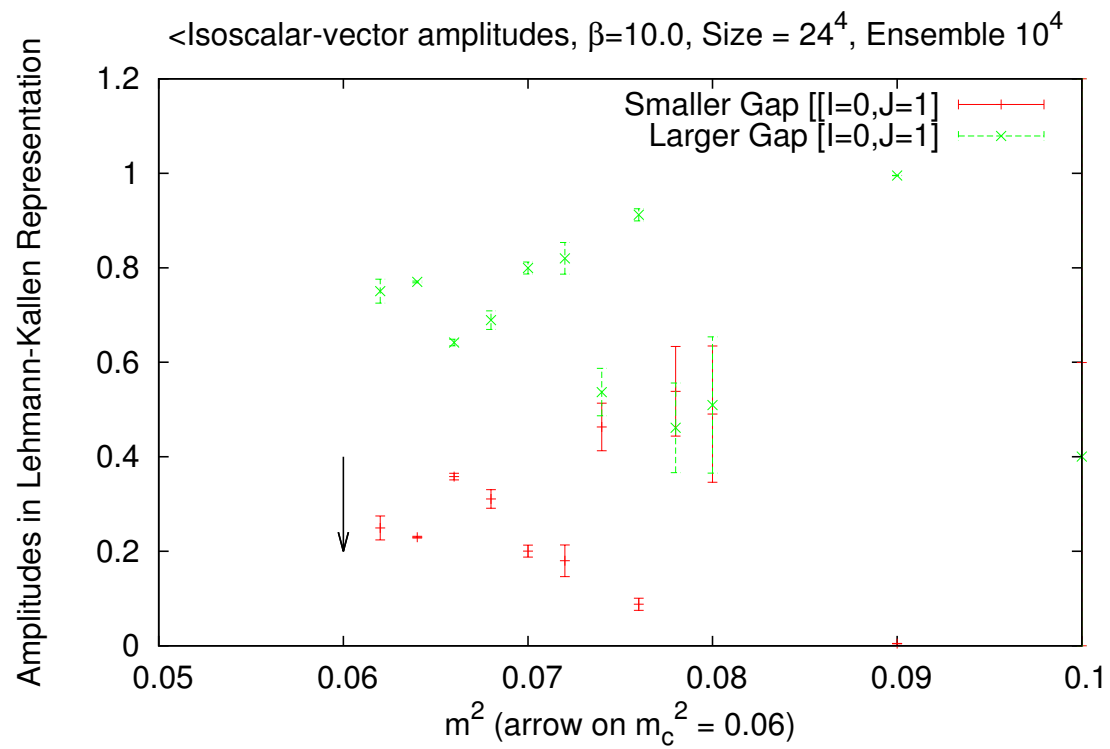Figure 10: **Weights in the isoscalar channel $(J = 0)$ for $\beta = 10$.**

Figure 11: **Weights in the isoscalar channel $(J = 1)$ for $\beta = 10$.**

10. Scaling?

In the limit $a = 0$ the parameter $m = Ma \to 0$, thus it is important if simulation supports scaling

$$\beta \sim \frac{1}{a}$$

For $\beta = 3$ the **Figures 12 and 13**, for $\beta = 10$ the **Figures 14 and 15**, and $\beta = 40$ the **Figures 16 and 17** illustrate the presence of scaling. That means that physical quantities have to be evaluated on the corresponding points.
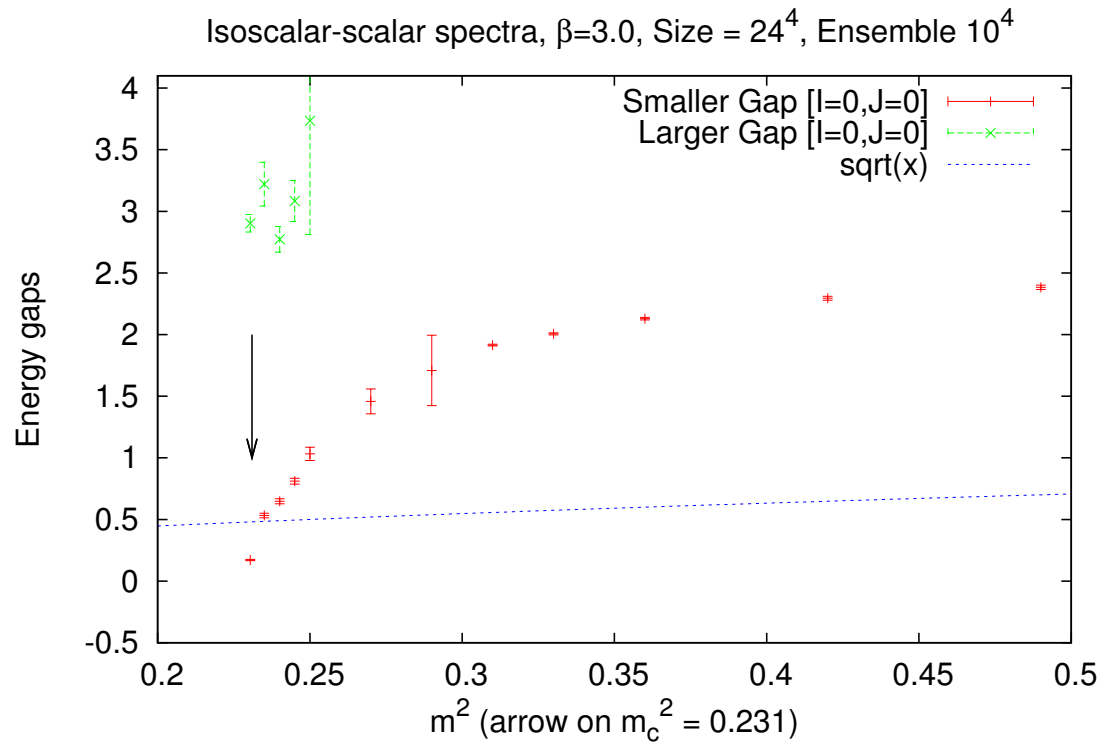
Figure 12: **Spectrum for $I = 0, J = 0$ for $\beta = 3$.**
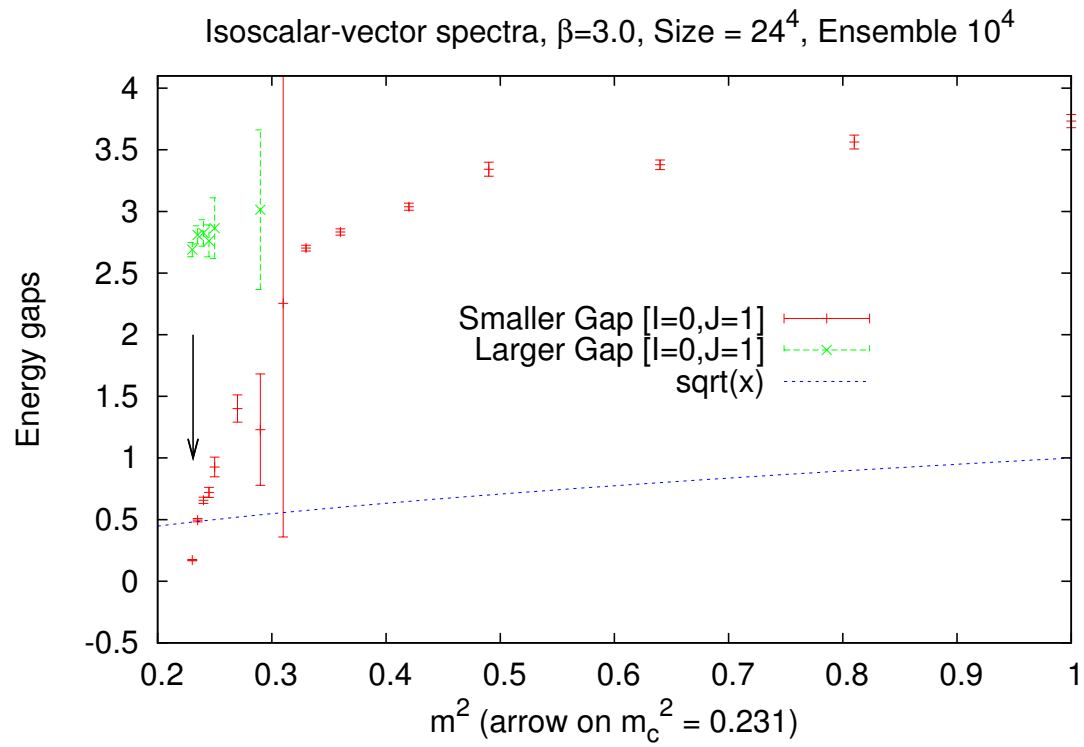
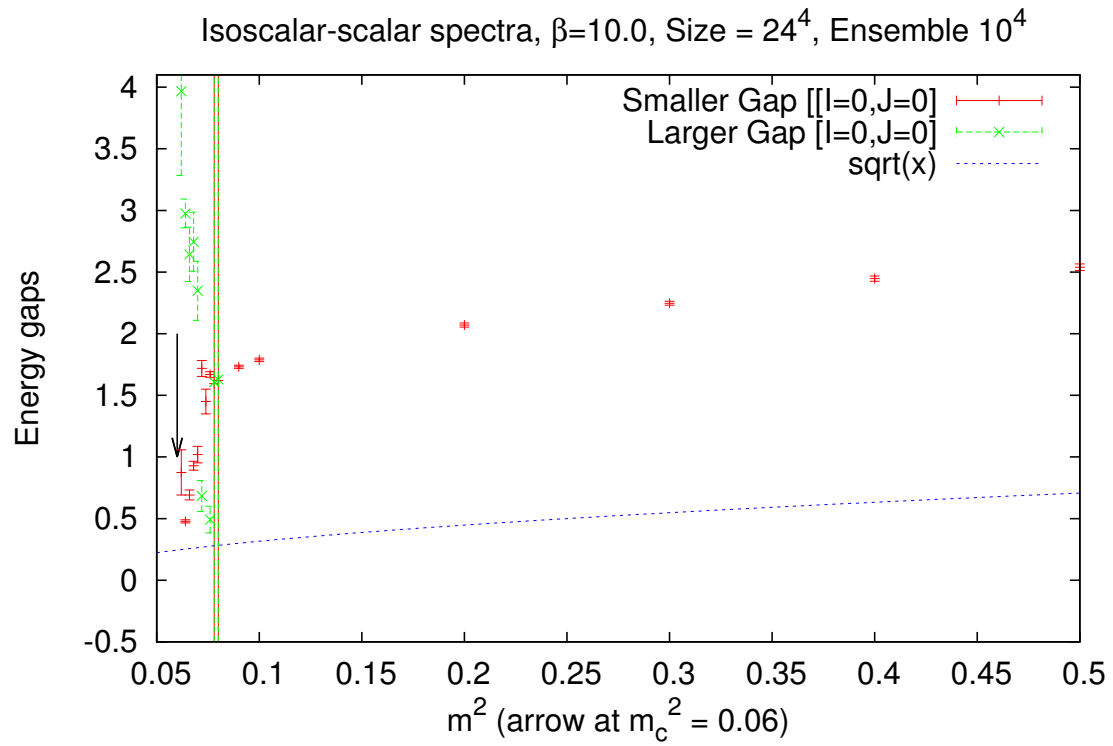Figure 13: **Spectrum for $I = 0, J = 1$ for $\beta = 3$.**

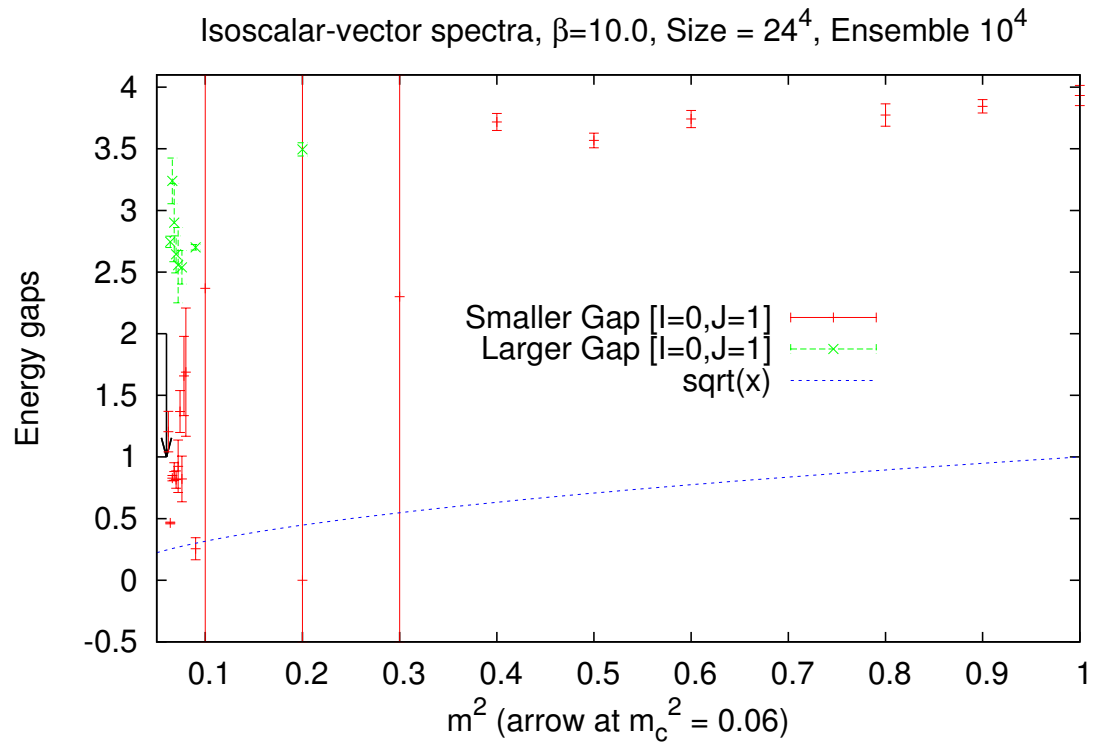Figure 14: **Spectrum for $I = 0, J = 0$ for $\beta = 10$.**

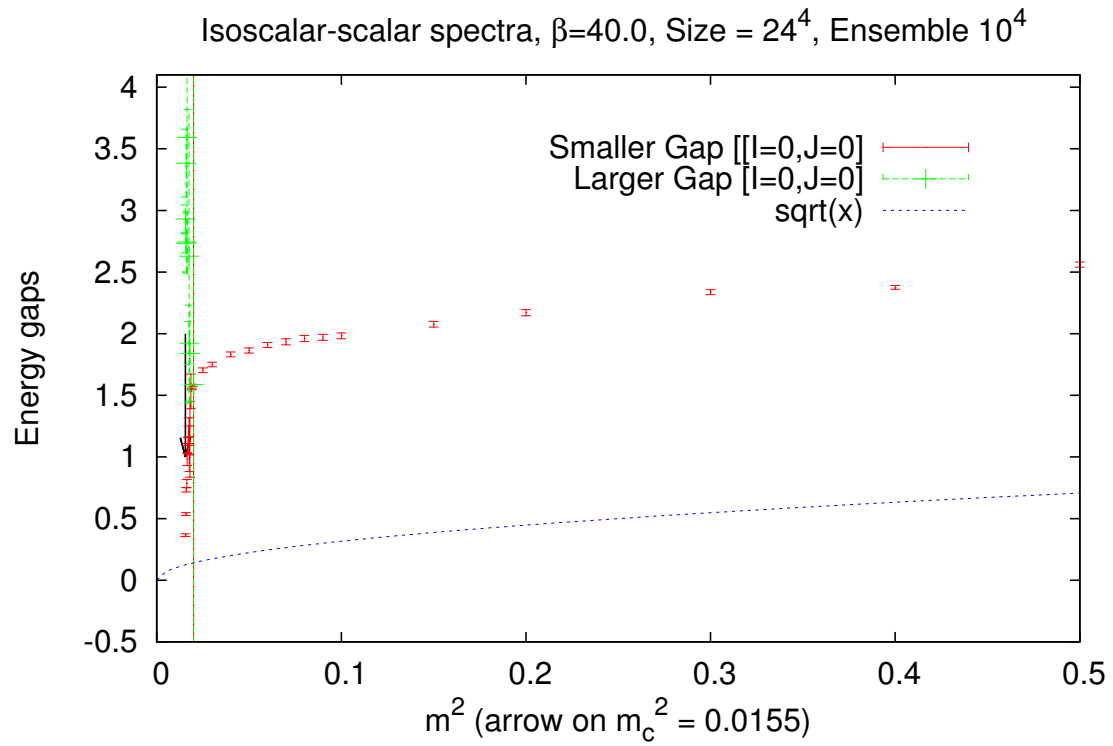Figure 15: **Spectrum for** $I = 0, J = 1$ **for** $\beta = 10$.

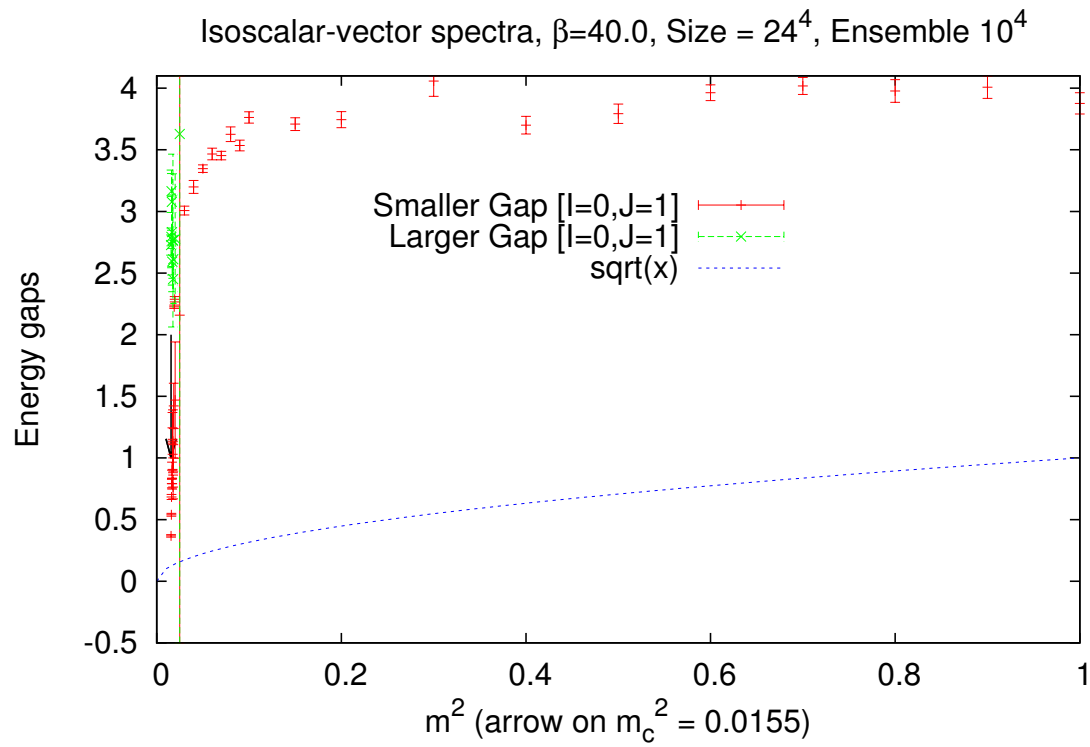Figure 16: **Spectrum for** $I = 0, J = 0$ **for** $\beta = 40$.

Figure 17: **Spectrum for** $I = 0, J = 1$ **for** $\beta = 40$.

11. Near the Transition Line

It is interesting to zoom near the Transition Line. We plot in the same figure the data for the gaps $(I = 1, J = 1)$, $(I = 0, J = 0)$ and $(I = 0, J = 1)$. From the Figures **18**, **19** and **20** we see that the energy levels come closer but they never reach a situation where a bound state is formed. The scalar sector is realized by resonances
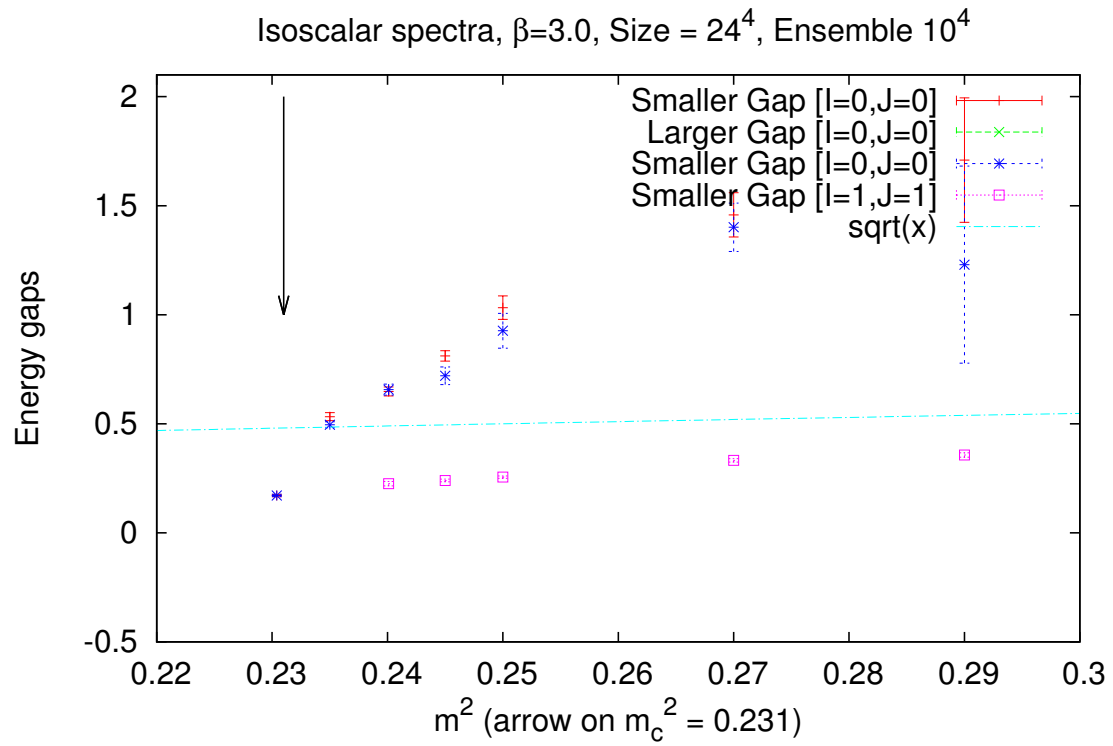
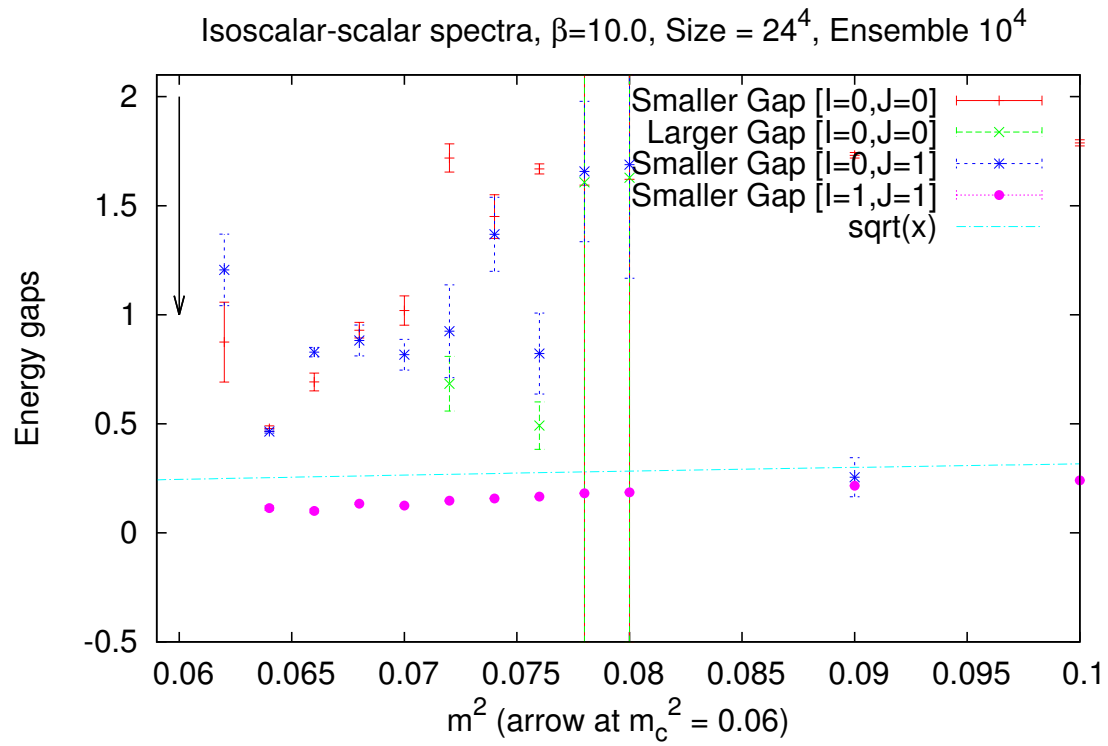Figure 18: **Zoom on the energy gaps near the TL for** $\beta = 3$**.**

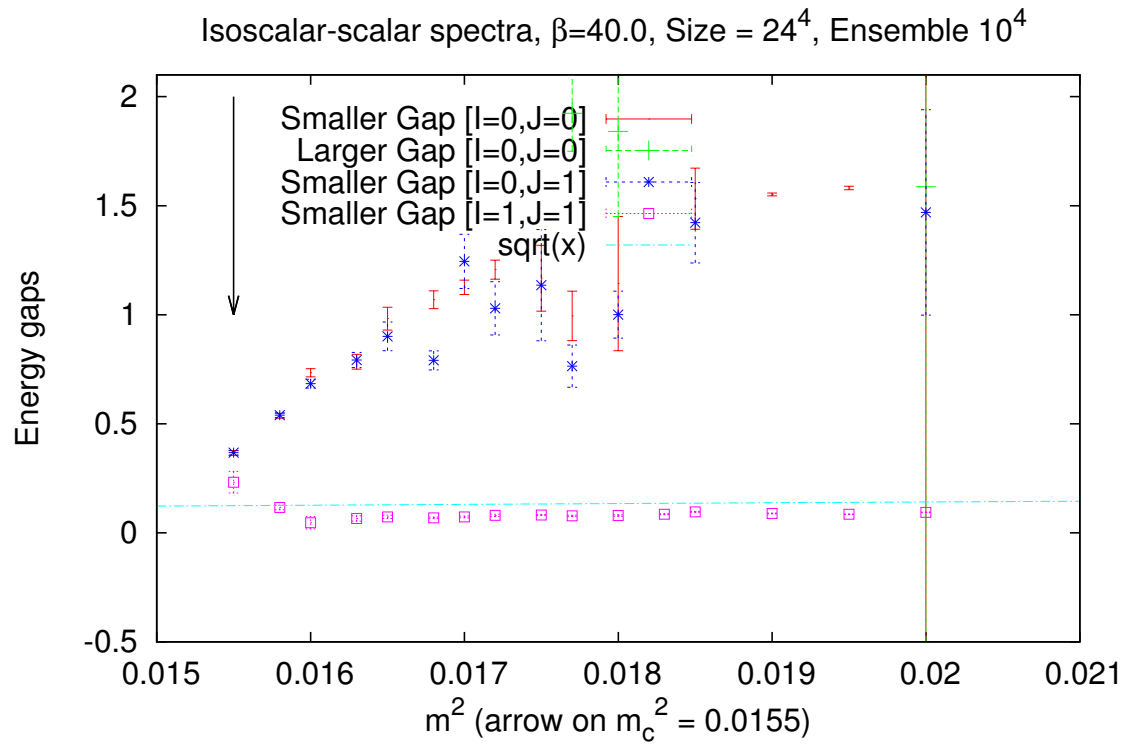Figure 19: **Zoom on the energy gaps near the TL for $\beta = 10$.**

Figure 20: **Zoom on the energy gaps near the TL for** $\beta = 40$.

12. Conclusions

i) No correlation in the $I = 1, J = 0$ channel $\smile$.

ii) Single exponential fit of correlators for $\beta < 2.2$ and for $m^2 >> m_c^2$. Bifurcation to two exponential fit for $m^2 \simeq m_c^2$.

iii) Scaling $(m \sim a^{-1}, \beta \sim a)$ seems working.

iv) The $I = 1, J = 1$ gap follows close the bare value m (gauge bosons).

v) There is a gap in the channel $I = 0, J = 0$ (the Higgs channel). However it is above threshold.

vi) There is a gap in $I = 0, J = 1$ almost degenerate with the "Higgs".

13. Outlook

1. Study the properties of the TL.

2. Examine the origin of the larger gap present after the bifurcation.

3. Improve the determination of the *phenomenological* line.

4. Survey the confined region (bounded by QCD line ($m^2 = 0$), Transition line and End Point).

References

[1] R. Ferrari, JHEP 0508, 048 (2005) [arXiv:hep-th/0504023].